Evaluation of Using a CCD Camera as a Versatile Measurement System for Flume Tank Observation

Chau-Chang Wang*, Po-Chi Chen†, Hsin-Hung Chen* and Wen-Li Chang*

*Institute of Applied Marine Physics and Undersea Technology
National Sun Yat-sen University, Kao-Hsiung, 804 Taiwan
Email: chauwang@mail.nsysu.edu.tw

† Taiwan Ocean Research Institute
National Applied Research Lab
3F, 106, Hoping E. Rd. Sec. 2., Taipei, 106 Taiwan

***Abstract*— A plane-based camera calibration method which substantially reduces the complexity of the procedure is presented in this paper. With the proposed method, camera array can be installed as a basic facility for wave flume tank experiment. Wave flume tank experiment is a methodology commonly used for ocean engineering research. Various parameters, such as wave properties on the surface (height, wave form, average level), current in the water (velocity field, vorticity and particle trace), bottom profile and sub-bottom layer thickness are measured with different apparatuses. Still image camera is one of the sensors widely used to extract information, such as waveform, bedform and velocity field (particle image velocimetry). The accuracy of image-based measurements mainly relies on the quality of the camera calibration which is a time-consuming process especially in field work. For the phenomena of interest observable on the flume tank window glasses, the features are planar in nature. Therefore, the camera calibration can be simplified as a map projection problem such that the time and efforts needed are reduced significantly while maintaining the desired accuracy. We studied the performance of the plane-based method by comparing the measurements with the theoretical values of a known curve which mimics a sandslope. The robustness of the method is examined by comparing the results acquired under the condition that the camera tripod and the quick-release are dissembled, assembled and repositioned during the experiments. According to the error analysis, the measurement can be accurate to less than 1. mm for static feature and 1 to 2 mm for dynamic feature.**

I. INTRODUCTION

Wave flume tank is a convenient facility commonly used for coastal and oceanic engineering research to study wave flow, wave breaking, sediment transport, scouring and internal wave [1], [2], [3]. Various parameters, such as wave properties on the surface (height, waveform, average level), current in the water (velocity field, vorticity and particle trace), bottom profile and sub-bottom layers are measured. Different instruments, electric- or optic-based, contact or non-contact, are developed to acquire temporal and spatial changes of these parameters. Capacitance wave gauge is a typical case of the electric-based methods; it provides the time series of the wave height at a single station [4]. To acquire a waveform, it is assumed that the waveform stays unchanged throughout the duration as it travels through the gauge. The time series of the wave height offers Eulerian observation of the wave. An alternative is to install an array of gauges with proper intervals to improve the resolution and quality of the measurement. Wave gauge need to be calibrated at the beginning of every experiment to have the correspondence between the water level and the output signal because the conductance of water may change. The procedure is easy, nevertheless, a necessary effort.

Particle image velocimetry (PIV), an optic-based approaches, is capable of measuring the velocity field [5]. It is gaining its popularity recently because it can provide the detailed structure of the velocity field. Moreover, it is non-intrusive. In other words, there are no issues like if the existence of the probe changes the pattern of the flow. In general, PIV uses CCD (charge couple device) cameras as the input devices to capture the images. If quantitative descriptions of the velocity field are desired, the camera needs to be calibrated. Calibration of a camera is to find the optical and the geometrical parameters of the imaging system. The optical parameters are focal length, distortion of lens, optical axis offset, CCD array linearity and etc; and geometrical parameters are position and orientation of the camera. Most calibration methods need a set of three-dimensional features with known coordinates as references, and solving a system of nonlinear equations to find out the parameters [6]. Although it is not necessary to calibrate the camera at the beginning of each experiment, the processes are time-consuming and delicate. Some of these parameters are very sensitive to the setup of the system, and a re-calibration is needed whenever the imaging system is disassembled or moved. In an ideal indoor condition it is already a non-trivial task. In practice, it is even more difficult to execute such a task in an environment like a flume tank facility.

For the phenomena of interest observable on the flume tank window glasses, the features are planar in nature. Therefore, the conventional full three-dimensional calibration are not needed. To convert the features described in the coordinates on the CCD sensory array (pixel coordinates) to the engineering coordinates on the window, a 2D mapping is required. Chen

978-1-4244-5222-4/10/$26.00 ©2010 IEEE

and Kak simplified the optical model and used a 4×3 constant transformation matrix to characterize this mapping [7]. Theoretically, only four points on the observation plane are required to determine the transformation matrix. This method is attractive because it does not involve any details of the optical and geometrical parameters of the model. On the other hand, because only one constant transformation matrix is applied over the entire image, the nonlinearity of the optics of the camera cannot be counted for in the entire field of view. Instead of this simplified linear mapping matrix, another approach is to use polynomial functions to relating a group of grid points on the observation plane to the their images in the pixel coordinates [8]. This approach is simple; however, for uneven distorted images, it is difficult to find appropriate polynomial functions to accurately characterize the nonlinearity.

We propose a modified plane-based camera calibration which was derived from a method used in calibrating the camera used in a laser line scanning systems [9]. The calibration can be simplified as a map projection problem such that the time and efforts needed is reduced significantly while maintaining the desired accuracy. The efficacy of this modified camera calibration method was verified in the development of a seafloor laser scanner [10]. In this paper, we adopt this plane-based method to calibrate cameras used for flume tank experiments and study the performance. The performance is demonstrated by comparing the measurements to the theoretical values of a known curves which mimic a sandslope. The robustness of the method is examined by analyzing the results acquired under the condition that the mounting tripod and the camera quick-release are dissembled and assembled and repositioned between two image acquisitions. The proposed measurement scheme will be referred as Measurement with Plane-based Calibrated Camera (MPCC) hereafter.

In this section, the advantages of using cameras as a quantitative observation device for flume experiments and motivation to modify the camera calibration are presented. In Section II the procedure of the plane-based camera calibration is described. The design of the calibration performance tests and the results are reported in Section III. Finally a conclusion is give in Section IV.

II. Plane-Based Calibration and Measurement

Before explaining the calibration method, we first review the concept of map projection. Map projection is a procedure to portray the surface of the earth or a portion of the earth on a flat surface. Consider a transparent hemisphere with meridian and parallel lines on its surface as shown in Fig. 1. We place a light source at the top of the hemisphere and a screen tangent to the south pole. The light rays project the terrain and the lines of longitude and latitude onto the screen to create the map. The lines of longitude and latitude serve as references to relate a point on the map with its location on the hemisphere. For a location which is not right at the intersection of a longitude line and a latitude line, we can estimate its coordinates from its distances to the neighboring longitude/latitude lines. Bearing this idea in mind, the CCD camera calibration for measuring features on a plane can be analogized to the projection problem: replace the projection screen with a CCD camera, and the transparent hemisphere with a board with known graticules placed coplanarly with the measurement plane. To decide the actual location of a point in the image, is just like reading a map to find out the location of a city.

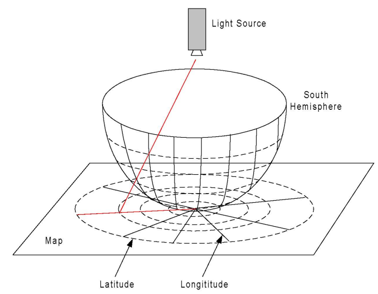

Fig. 1. The concept of map projection.

In this work, we used the plane-based calibration which was developed for calibrating the camera of an underwater laser scanning system [9]. The procedure is to place a calibration board coplanarly with the measurement plane which is the flume window glass in this case. The calibration board has a set of grid dots on its surface. A sample image of the calibration board captured by the CCD camera is shown in Fig. 2. The grid dots can be curve-fitted to create longitude and latitude lines such that the field of view of the camera is divided into smaller quadrangular regions. The dots on the calibration board are fabricated with known spacings. Therefore, their relative locations are assumed to be known parameters. For any target point sitting on a longitude (latitude) line, it shares the same horizontal (vertical) coordinate as the longitude (latitude) line. As for the other component of the coordinate, it can be estimated from its pixel distances to the neighboring latitude (longitude) lines. If the target point does not locate right on any longitude or latitude lines, its coordinates are decided by the ratios of the distances to the four sides surrounding it. The details regarding the algorithm, subpixel resolutions and accuracy of this method is available in [9]. In summary, the advantage of this method is: it involves neither intrinsic optic parameters (focal length, and distortion) of the CCD camera, nor the geometrical parameters (the relative position and orientation of the camera to the flume window glasses) of the setup. All non-linearities are lumped together and linearized separately for each quadrangle in the map. Furthermore, the simplicity and performance of this plane-based approach offer a convenient calibration feasible in the field work. This method was proved experimentally to have sub-mm accuracy when the measurement plane is one meter away with a CCD camera having 1024×768 pixels resolutions.

In this work, we used a similar configuration as in [9] but the laser scanning sheet was replaced by the flume observation

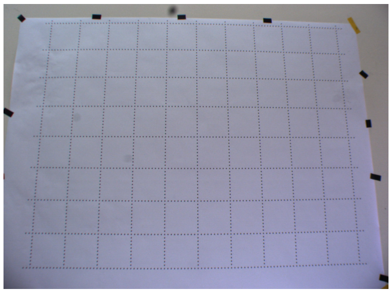

Fig. 2. The calibration board seen from the CCD camera.

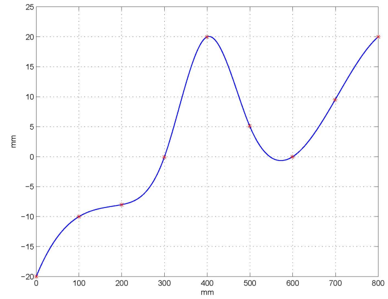

Fig. 3. A cubic spline passing nine controlled points (denoted as red stars) is used as a target to evaluate the performance of the proposed plane-based calibrated CCD measurement method. The vertical and horizontal axes are not to the same scale.

window glass. The CCD camera was placed at a proper distance to cover the entire scope of the window. Although the image acquired by the CCD camera may have distortions, the average resolution of the measurement was about 1 mm per pixel. If the resolution does not meet our need, we can either employ a camera of higher resolution or adopt a dual-camera setup to cover the entire window.

Prior to the experiments, the camera was mounted on a tripod head to take the image of a calibration board [1]. A sample image of the calibration board is shown in Fig. 2 on which the grid points are detected and characterized in the image pixel coordinates. The coordinates are then used to construct the mapping for the measurements. In theory, as long as the location and the orientation of the CCD camera remains unchanged throughout the experiments, the calibration board image can be taken after the experiment is finished; or multiple calibration images can be taken during the experiment to have redundancy. One point worth of noting is that in the laser scanning system, the laser light high signal-to-noise ratio which makes the measurements much robust to the variation of the environment. This is an advantage that the flume measurement does not have. To find out whether MPCC method functions well in the flume facility as in the laser scanning system, in the next section we present experimental results to answer the question with statistics.

III. Performance Analysis

In this section, we present three tests to help us to understand how the proposed plane-based approach performs in a flume facility environment. These tests were designed to find out key parameters, such as the effective scope and optical accuracy of the camera, the relation between the quality of the measurement and exactness of the camera mount, and the accuracy of the measurements compared to the wave gauge and ultrasonic altimeter readings.

A. Calibration Quality

The overall quality of the plane-based algorithm is attributed to two factors, the efficacy of the feature detection techniques used in the image post-processing and the effectiveness of the camera calibration. The former detects the desired features and describes them in pixel coordinates, while the latter answers for the accuracy of the coordinate transformation from from image unit (pixel) to the actual dimension (mm). We use a curve with known coordinates as a target and compare the difference between the measurements and the theoretical values of the curve. The results give an objective assessment over the portion which can be attributed to the latter factor. A curve, as shown in Fig. 3, is used as the test. It is a cubic spline which mimics the trend of a seabed. The cubic spline passes eleven control points denoted as red circles, and the slope at the end points are relaxed.

To expedite the experiment, we did not use numerical controlled milling machines to fabricate the desired pattern as in [9]. Instead, we used an HP Design 800ps printer to print out the calibration grid points and testing curves on paper. The resolution of the printer is 1200×2400 Dots Per Inch (DPI), and its ink nozzle position control is accurate to hundredth of a mm. It provides a cost-effective way to generate the desired pattern for calibration and tests.

The experiment procedures are as follows: First, the CCD camera (Basler cf102, 1388 x 1038) with a 14 mm lens was mounted on the quick-released cradle head of a tripod. The assembly was placed approximately one meter away from the measurement plane. Then the calibration sheet was placed tightly on the measurement plane, and its boundary was adjusted to fit in the scope of the camera. On the calibration sheet, the distance between two dots was 1 cm, and the dots were laid in vertical and horizontal line formations. Therefore, the scope of the camera was further divided into smaller square regions. The area enclosed between the four boundary lines is the effective workspace of the measurement. The camera lens was adjusted to focus on the plane to take the image of the calibration points. All the points were then used to extract the information needed for pixel to engineering unit conversion[9]. It should be noted that the orientation of the calibration grid was not aligned the camera optical axis. The procedure began with taking the image of the calibration sheet. Then the target curve sheet was placed onto the calibration sheet and scraped flat for taking the measurement image. The location and the orientation of the target sheet were not selected intentionally. The target curve sheet was randomly moved to anther location

[1] In practice, as long as the camera is not moved throughout experiment, the calibration image can be taken afterwards.

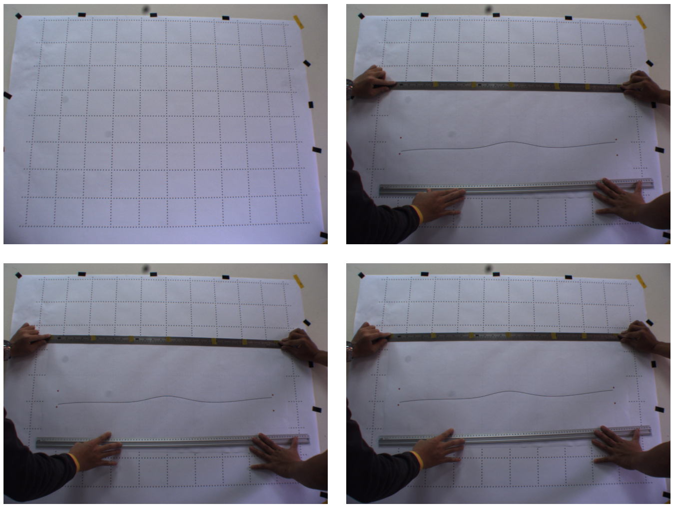

Fig. 4. A set of sample data which includes a calibration image and three curve images. On the curve image, there were four red dots, locating at (-5 30), (-5 -30), (805 30) and (805 -30) in the feature curve coordinate system, serve as references to translate and rotate the measurements to the theoretical curve coordinate system.

for taking another independent measurement of the target curve. Three measurements were defined as a set of data. In figure 4 we show a calibration image(the upper-left image) and three curve images(the other three in the figure). The preceding steps acquired one set of data. On the target curve, there were four dots with known location, which provide the references to restore the actual location and orientation for data comparison.

Upon the completion of acquiring one set of data, we took the camera assembly off from the quick-released cradle, and then put it back in. When we moved the camera assembly, extra cares were taken to make sure the overall position and configuration of the tripod remained *still*. By doing so, we simulated the scenario as in a flume facility: the camera is installed on a secure fixture for experiment and removed for instrument storage when experiment is finished. The same procedure was repeated ten times to have a statistics of the overall measurement performance. In Fig. 5 overlay the measurement on the theoretical value, as well as the difference between them. We can find that the error, for this specific case, is less than 1 mm everywhere. The statistics of the ten sets of the measurements tells us that the average error is less than 0.9 mm.

B. Flume Measurement

The ultimate goal of this work is to provide a method which is inexpensive, efficient and convenient to measure the waveform and seabed profile in a flume facility. A direct way to demonstrate the feasibility of the proposed method is to compare its measurement result with that acquired by the conventional instrument such as wavegauges for the same features. We performed experiments in a glass-walled wave flume located in the 3D Hydrodynamics Laboratory in the Department of Marine Environment and Engineering at Sun Yat-sen University, Taiwan. The flume is 42 m $\times$ 1.5 m $\times$ 1.5 m. It is equipped with a piston-type wave maker located at one end. The wave maker has a 0.7 m stroke, and is capable of generating waves in the period range 0.5 to 4 seconds with wave height up to 0.6 m at operating water depth of $d = 1.0$ m. The wave making is controlled by DHI Waves Synthesizer which is capable of generating first order Stock's waves and random waves of JONSWAP spectrum.

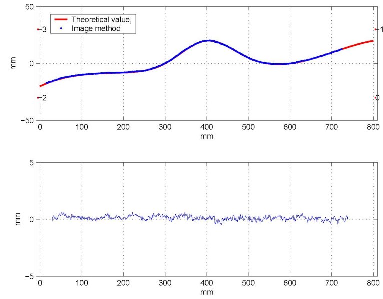

Fig. 5. The comparison between the measurement and the theoretical value of the target curve.

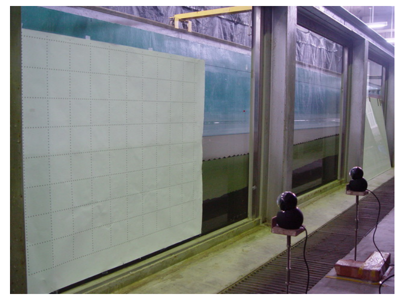

Fig. 6. A dual-cam setup for observing the flume window port.

We use capacitance wavegauges to measure waveform at multiple locations, and ultrasonic altimeter to measure seabed profile on a linear stage along the axis of the flume. For this paper, internet video conferencing cameras, 960 $\times$ 720, were used instead of professional quality CCD camera as the input devices to demonstrate the capacity of the proposed method. As shown in Fig. 6, videocams were mounted on a monopod. To have a one-mm per pixel resolution, the camera needed to be placed 70 cm from the flume window port. According to the geometry, the spatial resolution was about 0.8 mm^2 per pixel. The target features studied were sand bed (interface between sediment and water) and surface waves (interface between water and air).

1) Sand Slope Measurement: Initially, the sand bed was paved to be a 1/45 slope (Fig. 7). The sand bed appeared as a strong contrast interface in the image. A simple image processing technique, such as edge detection technique, can locate the boundary and characterize it in pixel coordinate. The same section of sand bed was also measured with ultrasonic altimeter at selected locations for comparison. In Fig. 8, the sand slope measured by the two approaches are overlaid on the same plot for comparison. The two measurements agree closely with error less than 1.0 mm for most of the locations. The magnitude of this discrepancy is just lightly larger than

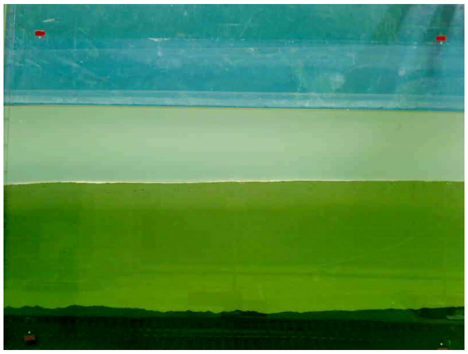

Fig. 7. A 1/45 sand slope paved for the experiment.

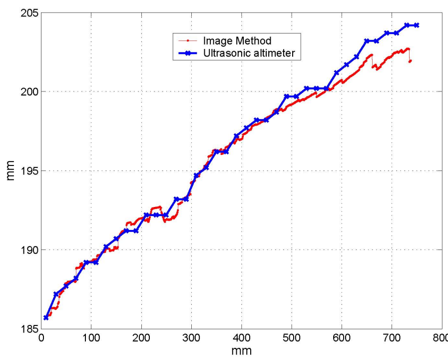

Fig. 8. The measurements comparison between MPCC method and an ultrasonic altimeter for the sand slope in Fig. 7.

that of the feature curve measurements in the previous section. The sand slope, after eight and half hours of wave action, evolved into a ripple field as shown in Fig. 9. The geometry of the sand bed was measured by both methods, and the results are overlaid on the same plot for comparison as shown in Fig. 10. The two measurements follow a similar trend but the details differ as much as 5.6 mm. This discrepancy might be unexpectedly eminent at the first glance because it is five times larger than the previous test. However, a side-view of the sand bed (Fig. 11) explains why there exists such a large discrepancy. The ripple field was actually two-dimensional. The crests and troughs were not straight lines parallel to each other but meandered across the sand bed. In other words, the measurement of the altimeter which was taken at the center of the tank was quite different from that by the window glass. Although this test does not provide useful information to discern the accuracy of our method, according to the result in the previous test, the actually geometry of the ripples should be in the similar error bound of the measurement.

2) Wave Measurement: A more challenging task is to measure the surface wave profile. Limited by the shutter speed of the internet webcam, the target wave velocity cannot be too fast otherwise the waveform image is not sharp, and the post processing will induce more uncertainties. We chose wave-making conditions to be wave period $T = 1.0$ sec and wave height $H = 2.0$ cm, such that the waveform image was of fair quality for post-processing. The flume was also equipped

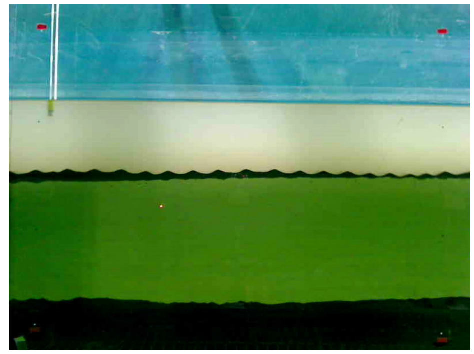

Fig. 9. The sand slope forms a ripple field on its surface after eight and half hours of wave action.

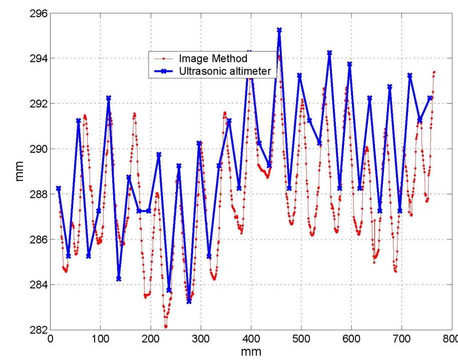

Fig. 10. The measurements comparison between MPCC method and an ultrasonic altimeter for the ripple field in Fig. 9.

Fig. 11. The sand slope after wave action forms a two-dimensional ripple field such that the measurements by the MPCC method differs a great extent from that by the altimeter along the center line of the flume.

with five capacitance wavegauges (labeled as W_1 to W_5 in Fig. 12) to measure the waveform synchronously. A snapshot of the waveform is shown in Fig. 12. Obviously that the waveform was not as sharp as the sand bed profile. A column of pixels (marked as the red line in Fig. 13) were selected for analysis. Their intensity (marked as the yellow solid line with red dots, not to scale) were overlaid on the image for reference. The intensity varied mildly from the air, through the vague boundary and into the water. There were about ten pixels in the transient zone. Unlike in the sand bed cases, the waveform profile does not exhibit a strong contrast. No significant discontinuity of the intensity level can be used to

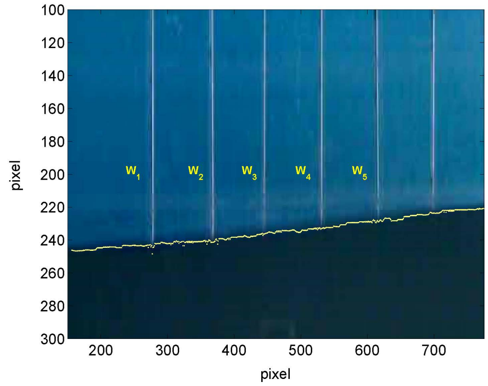

Fig. 12. The sand slope after wave action forms a two-dimensional ripple field such that the measurements by the MPCC method differs a great extent from that by the altimeter along the center line of the flume.

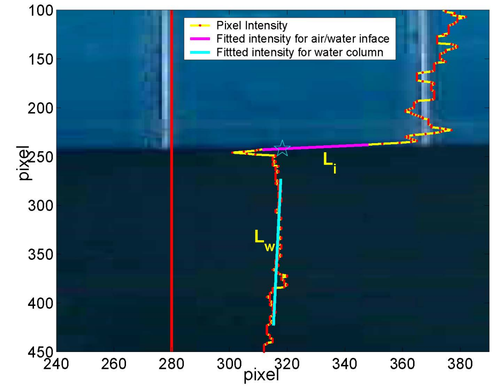

Fig. 13. The sand slope after wave action forms a two-dimensional ripple field such that the measurements by the MPCC method differs a great extent from that by the altimeter along the center line of the flume.

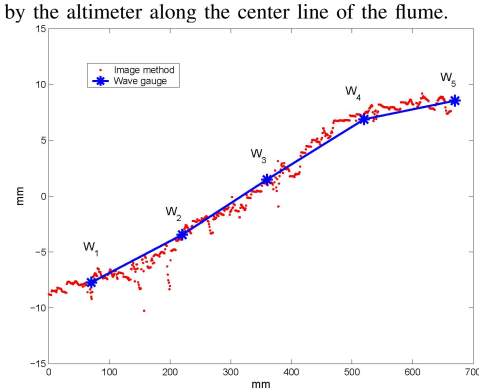

Fig. 14. The sand slope after wave action forms a two-dimensional ripple field such that the measurements by the MPCC method differs a great extent from that by the altimeter along the center line of the flume.

extract the location of the air/water interface. So simple edge detection techniques are not applicable here. Instead of using edge detection technique, the pixels in the interface (transient) zone and the water just beneath the air can be used to fit two straight lines. L_i stands for the general trend of the intensity varying from the air to the water; L_w tells the intensity trend in the water. It can seen that the pixel intensity for the area just a little further away from the interface was almost a constant value, while the pixel intensity the interface varies smoothly. However, the intersection of these two lines (denoted as a star) is relative stable which can be used to defined the elevation of water surface. This method was used to find the water surface for each column in the image, and the resulting surface is shown in Fig. 14. The wavegauge measurements, marked as blue stars, are translated to the image coordinate system for comparison. The measurement discrepancies are all less than 1 mm for the five locations. It should be noted that the wavegauges were also shown in the image. In the image, the wavegauges *dip* into the water surface, and they become distractions for the surface tracking algorithm. Even though the algorithm is robust enough to bring the tracking back to the water surface, it still leaves jumps in the measurement. This flaw will vanish when the measurement is carried out with the imaging method only.

IV. Conclusions

This paper provides an inexpensive method to measure the parameters for a flume tank. Calibration involves only simple image acquisition of the flume windows. Three experiments were carried out to assess the performance of the proposed method.

Acknowledgment

The authors would like to thank Miss J.Y. Wu, Mr. H.k. Chang and Mr. C.P. Chang for their assistance in the flume experiments, and Dr. C.P. Lee for the discussion in setting up the wave making conditions.

References

[1] I. L. Turner, P. E. Russell, and T. Butt, “Measurement of wave-by-wave bed-levels in the swash zone,” *Coastal Engineering*, vol. 55, no. 12, pp. 1237 – 1242, 2008.

[2] Y. Ryu and K.-A. Chang, “Breaking Wave Impinging and Greenwater on a Two-Dimensional Offshore Structure,” in *Proc. of The 5th Int. Offshore and Polar Engr. Conf.*, 2005, pp. 660–665.

[3] e. a. Cheng, L., “Three-dimensional scour below offshore pipelines in steady currents,” *Coastal Engineering*, vol. 56, no. 5-6, pp. 557–590, 2009.

[4] C. Keller, G. Irani, and R. Chapman, “A high-resolution, ocean wave gauge array system,” in *OCEANS 1984*, vol. 11, sep 1979, pp. 608 – 613.

[5] J. Fox and A. Patrick, “Large-scale eddies measured with large scale particle image velocimetry,” *Flow Measurement and Instrumentation*, vol. 19, no. 5, pp. 283 – 291, 2008.

[6] R. Tsai, “A Versatile Camera Calibration Technique for High-Accuracy 3d Machine Vision Metrology Using Off-the-Shelf TV Cameras and Lenses,” *IEEE Journal of Robotics and Automation*, vol. 3, no. 4, pp. 323–344, 1987.

[7] C. Chen and A. Kak, “Modeling and calibration of a structured light scanner for 3-D robot vision,” in *Proceedings of 1987 International Conference on Robotics and Automation*, vol. 4, 1989, pp. 807–815.

[8] D. Gujarati, *Basic Econometrics*. New York: McGraw-Hill, 2003.

[9] C. C. Wang and M. S. Cheng, “Nonmetric camera calibration for underwater laser scanning system,” *IEEE J. Oceanic Eng.*, vol. 32, pp. 383–399, 2007.

[10] C.-C. Wang and D. Tang, “Seafloor roughness measured by a laser line scanner and a conductivity probe,” *Oceanic Engineering, IEEE Journal of*, vol. 34, no. 4, pp. 459 –465, oct. 2009.